Liu *et al.*
Chinese Journal of Mechanical Engineering (2022) 35:90
https://doi.org/10.1186/s10033-022-00762-9

Chinese Journal of Mechanical Engineering

ORIGINAL ARTICLE

Open Access

Improved Dynamics Model of Locomotive Traction Motor with Elasticity of Rotor Shaft and Supporting Bearings

Yuqing Liu, Zaigang Chen*, Jieyu Ning, Kaiyun Wang and Wanming Zhai

Abstract

The locomotive traction motor is described as a rotor-bearing system coupling the kinetic equations of the traction shaft and its support bearings with the determination of their elastic deformations in this study. Under the effect of excitations induced by the dynamic rotor eccentric distance and time-varying mesh stiffness, the elastic structure deformations of the shaft and support bearings are formulated in the vibration environment of the locomotive. In addition, the nonlinear contact forces between the components of the rolling bearing, the lubricating oil film, and radial clearance are comprehensively considered in this study. The results indicate that the elastic deformations of the shaft and bearings can change the dynamic responses of the traction motor and its support bearings. There are large differences between the ranges of the rotor motion calculated by the rigid and the flexible traction motor models when the intensified wheel-rail interaction is considered. With the increase of the rotor eccentricity, the results underscore the role of the elasticity of traction shaft and support bearings in dynamic researches of the traction motor. The critical value of the initial eccentric distance for the rub-impact phenomenon decreases from 1.23 mm to 1.15 mm considering the flexible effect of the shaft and bearings. This dynamics model of the traction motor can provide more accurate and reasonable simulation results for correlational dynamic researches.

Keywords: Traction motor, Bearing, Gear mesh, Vehicle-track coupled dynamics

1 Introduction

The traction motor is the major power source of the locomotive, its dynamic characteristics directly affect the stability and safety of the vehicle. The internal dynamic forces induced by rotor eccentricity, which is caused by the bearing radial clearance and elastic structure deformations of the shaft and support bearings, can significantly influence the service status of the traction motor, especially for the motor with the static or dynamic eccentricity of the rotor [1, 2]. Besides, the dynamic loads induced by the vibration environment can increase the elastic structure deformations of the traction shaft and support bearings, which may challenge the stability and reliability of the traction motor, especially for the railway locomotive with intensified wheel-rail impact and gear mesh. Therefore, to accurately evaluate the dynamic characteristics of the traction motor and its support bearings during the operation of the locomotive, it is essential to propose a dynamic modeling method considering the elasticity of the traction shaft and bearings.

The rolling bearing is the key component of the traction motor, which is used to support the rotor and reduce the friction effect between the rotor and stator. Many works were presented to investigate the dynamic characteristics of the rolling bearing. Gupta [3] analyzed the skidding phenomenon of the balling bearing considering the elastohydrodynamic lubrication effect. Yang et al. [4] used a substructure mode synthesis method to simulate the flexibility of the cage and established a rigid-flexible dynamics model for a cylindrical bearing. Liu et al. [5]

*Correspondence: zgchen@home.swjtu.edu.cn

State Key Laboratory of Traction Power, Southwest Jiaotong University, Chengdu 610031, China

analyzed the skidding phenomenon of the rolling bearing where the cage was discretized into several segments so as to introduce the flexibility of the cage. Recently, Liu et al. [6] presented a lumped-mass dynamics model to investigate the dynamic and acoustic characteristics of a defective bearing. In addition, the structural deformations of the components of the bearing under the radial load have attracted much attention. Jones [7] proposed a general theory for calculating elastic compliances of a rolling bearing under any radial loads. Based on the Discrete Element Method, Machado et al. [8] established a bearing dynamics model with elastic rings. Liu et al. [9] established a finite element model of the rolling bearing considering the elastic deformation of the roller, inner and outer rings. For improving the calculating efficiency, Liu et al. [10] further proposed a numerical analytical method. The results indicated that the elastic deformation of the components can significantly affect the vibration of the bearing. The analytical methods given by Refs. [10, 11] can provide important theoretical guidance for formulating the uniform centrifugal expansions and compression deformations of rollers and rings induced by the rotational speed and load distribution of bearing.

The traction motor can be regarded as a typical rotor-bearing system. Over the years, works on the rotor-bearing system have resulted in a number of improvements. Ehrich et al. [12, 13] performed investigations on the effect of the bearing radial clearance on the vibration of the rotor-bearing system. Villa et al. [14] analyzed the effects of the radial clearance and internal interactions between the components of the ball bearing on the stability and dynamic behavior of a flexible rotor-bearing system. Shi et al. [15] took the structural arrangement, rotor mass unbalance and bearing parameters (e.g., the radial clearance and roller length) into account in a vertical rotor-bearing system dynamics model. Based on Gupta's bearing model [16], Li et al. [17] proposed a dynamic model method for a ball bearing-rotor system. And the finite element method was adopted to calculate the elastic deformation of the rotor. Based on Green's function, Tan et al. [18] proposed a rotor-bearing dynamic modeling method with electromechanically coupled boundary conditions to analyze the performance of the ring-shaped piezoelectric damper. In addition, in order to analyze the rub-impact phenomenon of the hydraulic generating set, Zhang et al. [19] established a corresponding rotor-bearing dynamics model considering both static and dynamic eccentricities. In the above, the effects of structural parameters of the varying support bearings and the nonlinear characteristics of the rotor-bearing system are deeply studied. However, the dynamic responses of the rotor-bearing system under the time-varying external excitations (e.g., the equipment vibration environment, time-varying gear mesh force, and so on) are not comprehensively considered.

During the operation of a locomotive, the traction torque is transmitted from the traction motor to the wheel-rail interface via the gear engagement. In addition, the traction motor is hung on the bogie through the suspension units and supported by the wheelsets via the axle-hung bearings. Therefore, the dynamic behavior of the traction motor has a close connection with the wheel-rail impact through gear engagement and structure vibration transmission. The time-varying mesh force of the gear pair makes the traction motor bear a periodical load in the vibration environment of the locomotive. For investigating the wheel-rail interactive mechanism and the effect of internal excitations in power transmissions on the dynamic behaviors of the vehicle system, many researchers have carried out a wide range of work. Huang et al. [20] analyzed the dynamic responses of the gear transmission of a high-speed train by using the software SIMPACK. Based on the typical vehicle-track coupled dynamics model [21], Chen et al. [22] made the gear transmission incorporate into the coupled system via the gear engagement and wheel-rail interaction. Yu et al. [23] investigated the vibration responses of the frame-mounted traction motor during the operation. Zhou et al. [24] extracted the fault feature of the wheel flat from the current signal of the traction motor via the electromechanical coupling effect. However, in these researches, the traction motor is regarded as a mass block and the internal interactions of the motor and its support bearings are ignored. Actually, the working conditions of the traction motor cannot be fully reflected. Fortunately, Wang et al. [25] and Liu et al. [26] respectively established the spatial vehicle-track coupled dynamics model for a high-speed train and a locomotive considering the mechanical structures of the traction motor and track irregularity, and the thermal and dynamic characteristics of the motor bearings were analyzed, respectively. In addition, Liu et al. [27] further investigated the vibration responses of the traction motor with surface waviness on races of its driving end bearing. Based on the above descriptions, the dynamic researches about the traction motor under the internal and external excitations of the railway vehicle have gained researchers' attention. However, it should be noted that, compared with the mature rotor dynamics, the relative research is still in very preliminary status, and the interactive mechanism between the traction motor and vehicle-track system is not fully clear. The recent researches chiefly focused on the improvement of accuracy of loads acting on the traction motor in the vibration environment of the locomotive. The components of the traction motor are regarded as rigid bodies, while the elastic deformations of the rotor

and support bearings induced by the radial loads are ignored. The rotor eccentricity is generated by the bending of the shaft, assembling error, radial clearance of the support bearings, and so on. It is worth that the large gear mesh force, the gravity of the rotor and the internal dynamic forces of the motor can aggravate the bending of the shaft and internal elastic deformations of the rolling bearings. To overcome the gap, this study is reported to propose an improved dynamics model of traction motor considering the elastic deformations of the traction shaft and support bearings.

A rotor-bearing-pinion dynamics model of the locomotive traction motor has been improved by coupling the kinetic equations of the rotor and its support bearings with the determination of elastic deformations in this study. In this model, the complete mechanical structures of the traction motor and its support bearings are considered, and the traction motor is regarded as a rotor-bearing-pinion system with the elasticity of traction shaft and support bearings. Under the excitations induced by the track irregularity, time-varying mesh stiffness and dynamic rotor eccentricity, the elastic deformations of the traction shaft and support bearings are formulated. In addition, the nonlinear contact forces generated at the roller-race and roller-cage interfaces, the corresponding friction forces, the radial clearance of the motor bearings are comprehensively taken into account in this study. The proposed flexible traction motor dynamics model can provide more accurate and rational simulation results for the dynamic researches about the traction motor during the operation.

2 Dynamic Model Formulation

As illustrated in Figure 1, the traction motor consists of a rotor, a traction shaft and two support rolling bearings. The rotor and pinion are both fixed on the traction shaft. The driving and non-driving end bearings are installed by the rotor symmetrically, with shorter and longer distances from the pinion, respectively. Therefore, the traction motor can be regarded as a rotor-bearing-pinion system considering the elasticity of the traction shaft and support bearings. During the operation of the locomotive, time-varying mesh forces (F_m) and internal dynamic forces (F_r) of the traction motor induced by the dynamic eccentricity of rotor, namely, the centrifugal force, unbalanced magnetic pull (UMP), and rub-impact force, simultaneously act on the traction motor system. In addition, the structure vibrations of the vehicle system excited by the track irregularity can significantly intensify the gear mesh and generate large dynamic loads. Considering the complex mechanical structures of the bearing, the time-varying support stiffnesses of the motor bearings induced by the different numbers of rollers in the loaded region can cause the time-varying resultant forces generated from the roller-race interface and lead to the periodic vibration of the traction motor. The flexible deformations between the roller and the races can transmit the interactive forces between the rotor and motor.

To obtain the accurate dynamic loads and analyze the dynamic responses of the traction motor, a locomotive-track spatially coupled dynamics model established by Liu et al. [26] is adopted in this study. In this model, the locomotive is composed of the car body, bogie frame, wheelset, and traction power transmission. All components of the locomotive and corresponding connection elements are regarded as rigid bodies and spring (K) -damper (C) elements, respectively. The traction motor is hung on the bogie frame and mounted on the wheelset through the hung rod and hugging bearings, respectively. It should be noted that the multiple-rigid-body model of traction motor established in Ref. [26] is replaced by the proposed dynamics model of traction motor in this study. The schematic diagrams of the locomotive and its traction system are illustrated in Figure 2. The traction power is transmitted from the traction motor to the wheel-rail interface via the elastic deformations of the gear pair represented by a spring-damper element (K_m and C_m) along the line of action. The traction power transmission and the locomotive are coupled through the gear engagement

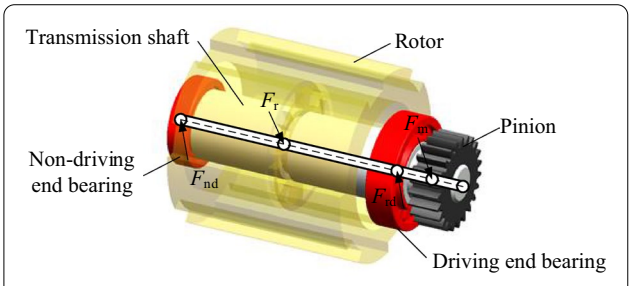

Figure 1 Schematic diagram of the locomotive traction motor

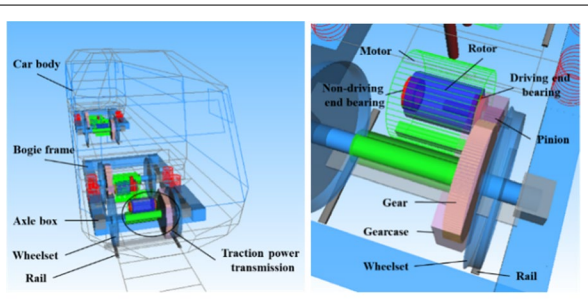

Figure 2 Schematic diagrams of: **a** the locomotive and **b** its traction power transmission

and wheel-rail interaction. In addition, the flexibility of the rail is described by the Euler beam. The track irregularity is the major external excitation for this locomotive-track coupled system. More detailed information about this dynamics model can be found in Refs. [26–30].

2.1 Elastic Deformation of the Transmission Shaft

As illustrated in Figure 1, under the time-varying mesh force, dynamic forces of the rotor (e.g., the centrifugal force, UMP, and rub-impact force), and radial resultant forces of the support bearings, the traction shaft of the traction motor can be regarded as an elastic composite beam composed of the simply supported beam and the cantilever beam. The elastic deformations of the traction shaft are coupled with the kinetic equations of the rotor in this study. The schematic diagram of the traction shaft is illustrated in Figure 3. L_1 and L_2 are the lengths of the simply supported beam and cantilever beam, respectively. a and c are the lateral distances of action points between the dynamic force of the rotor/mesh force and the driving/non-driving end bearing, respectively.

Based on the mechanics of materials, the relation between load and deflections of this elastic composite beam is deduced in this section. The approximately differential equation of the flexural curve of the traction shaft can be expressed as

$$EI\ddot{w} = \begin{cases} F_{\mathrm{nd}}x & 0 \le x \le a, \\ F_{\mathrm{nd}}(x-a) - F_{\mathrm{r}}x & a < x \le L_1, \\ F_{\mathrm{nd}}(x-a) - F_{\mathrm{r}}x - F_{\mathrm{d}}(x-L_1) & L_1 < x \le L_1 + c, \\ F_{\mathrm{nd}}(x-a) + F_{\mathrm{m}}(x-L_1-c) - F_{\mathrm{r}}x - F_{\mathrm{d}}(x-L_1) & L_1 + c < x \le L_1 + L_2, \end{cases} \tag{1}$$

where E and I are the elastic moduli and inertia moment of the traction shaft, respectively; F_{r}, F_{m}, F_{d} and F_{nd} are the dynamic forces of the rotor, mesh force, and support forces of the driving and non-driving end bearings, respectively.

The deflection equation of the traction shaft can be deduced as

$$EIw = \begin{cases} -\frac{1}{6}F_{\mathrm{nd}}x^3 + B_1x + B_2 & 0 \le x \le a, \\ \frac{1}{6}F_{\mathrm{nd}}(x-a)^3 - \frac{1}{6}F_{\mathrm{r}}x^3 + C_1x + C_2 & a < x \le L_1, \\ \frac{1}{6}F_{\mathrm{nd}}(x-a)^3 - \frac{1}{6}F_{\mathrm{r}}x^3 - \frac{1}{6}F_{\mathrm{b}}(x-L_1)^3 + D_1x + \mathrm{D}_2 & L_1 < x \le L_1 + c, \\ \frac{1}{6}F_{\mathrm{nd}}(x-a)^3 + \frac{1}{6}F_{\mathrm{m}}(x-L_1-c)^3 - \frac{1}{6}F_{\mathrm{r}}x^3 & \\ -\frac{1}{6}F_{\mathrm{d}}(x-L_1)^3 + E_1x + E_2 & L_1 + c < x \le L_1 + L_2, \end{cases} \tag{2}$$

where B_1, B_2, C_1, C_2, D_1, D_2, E_1 and E_2 are the calculated coefficients according to the actual support mode of bearings in traction motor, which can be calculated as

$$\begin{cases} B_1 = C_1 = D_1 = E_1 = \frac{F_{\mathrm{a}}L_1^3 - F_1(L_1-a)^3}{6L_1}, \\ B_2 = C_2 = D_2 = E_2 = 0. \end{cases} \tag{3}$$

The elastic deformations of the traction shaft at the positions of rotor and pinion can be calculated by Eqs. (2) and (3) when x is equal to a and L_1+c, respectively.

2.2 Elastic Deformation of Roller Bearing

Compared with the rigid bearing, the global deformations of the elastic components are composed of the elastic compression deformations of the roller and races at the contact area, the uniform centrifugal expansion caused by the rotating speed, and the structure distortion due to the load distribution. Taking the global deformation of the roller (δ_{r}) as an example, which is illustrated in Figure 4, δ_{c}, δ_{er} and δ_{dr} are the elastic compression deformation, centrifugal expansion and the structure distortion of the roller. For the traction motor, the rolling bearings are installed between the rotor and motor to support the rotor and reduce the corresponding friction effect. The inner and outer rings are fixed on the rotor and motor respectively. Therefore, the expansions of the external race of the inner ring, internal race of the outer ring, and rollers are considered in this study. The interactive forces between the rotor and motor are transmitted via the rollers which are regarded as spring elements (K_{e}) in the radial direction.

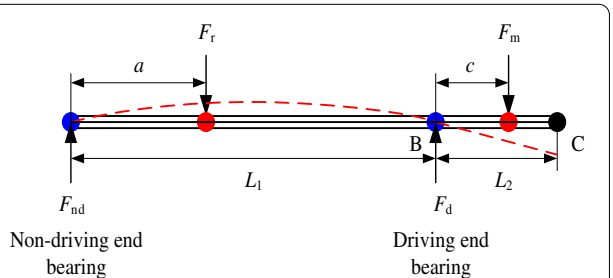

Figure 3 Schematic diagram of the elastic transmission shaft

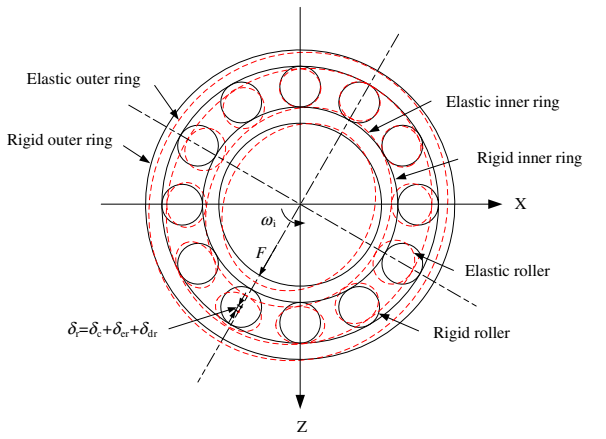

Figure 4 Comparison between the rigid and elastic rolling bearings

Based on the Hertz contact theory, the compressive deformation between the roller and inner/outer race can be respectively expressed as [31]

$$\begin{cases} \delta_{ci} = \frac{2Q_i}{\pi l_r}\frac{1-\nu^2}{E_e}\left(\ln\frac{4R_iR_r}{b_i^2}+0.814\right) & \text{for roller - inner race,} \\ \delta_{co} = \frac{2Q_o}{l_r}\frac{1-\nu^2}{E_e}(1-\ln b_o) & \text{for roller - outer race,} \end{cases} \tag{4}$$

where Q and b are the contact forces and semi-widths of the contact area between the roller and inner/outer races, respectively; the subscript i and o denote the inner and outer race, respectively; l_r is the equivalent length of the roller; E_e and ν are the equivalent elastic modulus and Poisson's ratio, respectively; R_i and R_r are the radii of the inner race and roller, respectively.

The expansion and distortion of the roller can be respectively expressed as [32, 33]

$$\begin{aligned} \delta_{er} =& \frac{(1+\nu_r)(3-2\nu_r)}{8E_r(1-\nu_r)}\rho_r\theta_r^2R_r\left[(1-2\nu_r)-\frac{1-2\nu_r}{3-2\nu_r}\right]R_r^2 \\ &+\frac{1+\nu_r}{E_r}Q_r(1-2\nu_r), \end{aligned} \tag{5}$$

$$\begin{aligned} \delta_{dr} =& \frac{Q_r}{l_rR_{r1}E_r}\left[\frac{R_{r1}}{2}\left(\frac{\pi}{4}-\frac{2}{\pi}\right)\right. \\ &\left.+\frac{R_{r1}}{2}\left(\frac{4}{\pi}-\frac{\pi}{4}+\frac{\pi\zeta E_r}{4G_r}\right)-\frac{R_{r1}}{\pi}\right], \end{aligned} \tag{6}$$

where E and ν are the elastic module and Poisson's ratio of the material, respectively; ρ is the density; θ is the rotational speed; the subscript r represents the roller; Q_r contact force between the roller and race; R_{r1} is the radius of the deformed roller; ζ is the coefficient for the roller cross-section profile; G is the tangential elastic modulus.

For the flexible inner and outer rings, the global deformations of the flexible race at the contact angular position ψ can be respectively expressed as [10]

$$\delta_{gi}(\psi) = 0.5\delta_{ei} + \delta_{di}(\psi) + 0.5\delta_{ci}, \tag{7}$$

$$\delta_{go}(\psi) = 0.5\delta_{eo} + \delta_{do}(\psi) + 0.5\delta_{co} \tag{8}$$

where δ_{ei}/δ_{eo}, δ_{di}/δ_{do} and δ_{ci}/δ_{co} are the expansion, distortion, and compression deformations of the inner/outer rings, respectively.

The expansion of the external face of the inner ring and the internal face of the outer ring can be respectively expressed as [34]

$$\begin{aligned} \delta_{ei} =& \frac{\rho_i\omega_i^2}{4E_i}\left[(1-\nu_i)(3+\nu_i)\left(R_{i1}^2-R_{o1}^2\right)\right. \\ &\left.+(1+\nu_i)(3+\nu_i)R_{i1}^2-\left(1-\nu_i^2\right)R_{o1}^2\right]R_{o1}, \end{aligned} \tag{9}$$

$$\begin{aligned} \delta_{eo} =& \frac{\rho_o\omega_o^2}{4E_o}\left[(1-\nu_o)(3+\nu_o)\left(R_{i2}^2-R_{o2}^2\right)\right. \\ &\left.+(1+\nu_o)(3+\nu_o)R_{o2}^2-\left(1-\nu_o^2\right)R_{i2}^2\right]R_{i2}, \end{aligned} \tag{10}$$

where ω is the rotational speed of the race; R_1 and R_2 are the internal and external radii of the ring, respectively.

The distortion of the inner or outer ring at the contact angular position ψ can be expressed as [35]

$$\delta_d(\psi) = W(\psi)(K_0 + K_1\cos\psi + K_2\cos 2\psi), \tag{11}$$

where $W(\psi)$ is the radial and single load; K_0, K_1 and K_2 are the stiffness coefficient parameters.

Considering the effect of the lubricating oil, the central film thickness between the roller and race can be expressed as [36]

$$h_{cf} = 3.533\frac{l_r^{0.13}R_e^{0.43}\alpha^{0.54}(\eta_0\mu)^{0.7}}{E_e^{0.03}Q_r^{0.13}}, \tag{12}$$

where R_e is the roller-race equivalent radius; α and η_0 are the viscosity pressure and kinetic viscosity coefficients for the lubricating oil, respectively; μ is the mean velocity between the roller and race.

For the lubricated rolling bearing, the equivalent contact stiffness between the inner and outer races via the roller can be expressed as

$$K_{er} = \frac{1}{\frac{1}{K_{dr}}+\frac{1}{K_{cr}}+\frac{1}{K_{cf}}}, \tag{13}$$

where K_{dr}, K_{cr}, and K_{cf} are the body stiffness of the roller, the contact stiffness between the roller and race, and the lubricating oil stiffness, respectively.

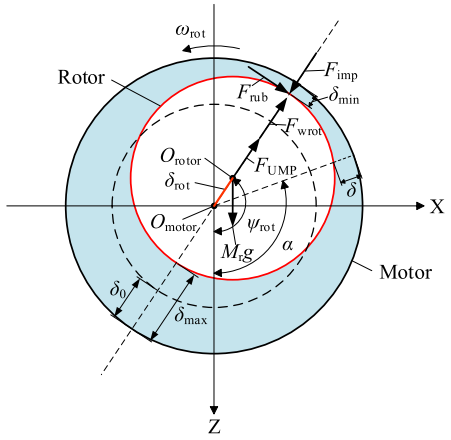

Figure 5 Schematic of the rotor eccentricity

More detailed information about the flexible rolling bearing can be referenced in Refs. [10, 31–36].

2.3 Internal Dynamic Forces of the Traction Motor

During the operation of the traction motor, the dynamic eccentricity of the rotor is inevitably generated owing to the elastic deformation of the traction shaft and the compression deformations between the roller and races under the dynamic loads acting on the motor bearings. The schematic of the rotor eccentricity is illustrated in Figure 5. The dynamic rotor eccentricity can induce the centrifugal force, UMP, gravity torque, and even the rub-impact forces.

Considering the rigid displacement of the rotor and elastic deformation of the traction shaft, the actual eccentricity of the rotor can be expressed as

$$\delta_{rot} = \sqrt{(X_{rm} + w_{rx} + e_{rot}\sin\psi_{rot})^2 + (Z_{rm} + w_{rz} + e_{rot}\cos\psi_{rot})^2}, \tag{14}$$

where X_{rs} and Z_{rs} are the relative rigid displacements between the roller and motor in longitudinal and vertical directions, respectively; w_{rx} and w_{rz} are the elastic deformations of the shaft at the rotor position in longitudinal and vertical directions, respectively; e_{rot} is the initial eccentricity of the rotor. The actual angular position of the rotor ψ_{rot} is determined by the rotational and planer displacements of the rotor and motor.

Consequently, the centrifugal force and gravity torque of the rotor can be respectively expressed as

$$F_{wrot} = M_{rot}\omega_{rot}^2\delta_{rot}, \tag{15}$$

$$T_{gr}=M_{rot}g\delta_{rot}\sin\psi_{rot}, \tag{16}$$

where M_{rot} is the mass of the rotor; ω_{rot} is the rotational speed of the rotor; g is the gravitation constant.

Based on the discussion in Refs. [37, 38], for a two-pole pair traction motor which is widely employed in the railway vehicle, the UMP induced by the eccentric rotor in longitudinal and vertical directions can be expressed as

$$\begin{aligned} F_{UMPx} =& f_1\cos\psi_{rot} + f_{3c}\cos(2\omega_{rot}t - 3\psi_{rot}) \\ &+ f_{3s}\sin(2\omega_{rot}t - 3\psi_{rot}) \\ &+ f_{4c}\cos(2\omega_{rot}t - 5\psi_{rot}) \\ &+ f_{4s}\sin(2\omega_{rot}t - 5\psi_{rot}), \end{aligned} \tag{17}$$

$$\begin{aligned} F_{UMPz} =& f_1\sin\psi_{rot} + f_{3c}\sin(2\omega_{rot}t - 3\psi_{rot}) \\ &- f_{3s}\cos(2\omega_{rot}t - 3\psi_{rot}) \\ &- f_{4c}\sin(2\omega_{rot}t - 5\psi_{rot}) \\ &+ f_{4s}\cos(2\omega_{rot}t - 5\psi_{rot}), \end{aligned} \tag{18}$$

where the calculating method for coefficients f_1, f_{3c}, f_{3s}, f_{4c} and f_{4s} has been proposed in Ref. [37].

If the rotor eccentric distance is larger than the air gap δ_0 of the traction motor, the rub-impact phenomenon will be formed between the rotor and motor. The corresponding rub and impact forces can be expressed as

$$F_{imp} = \begin{cases} K_{rm}(\delta_{rot} - \delta_0) & \delta_{rot} \geq \delta_0, \\ 0 & \delta_{rot} < \delta_0, \end{cases} \tag{19}$$

$$F_{rub}=\mu_{rm}F_{imp}, \tag{20}$$

where K_{rm} is the contact stiffness between the rotor and motor; μ_{rm} is the friction coefficient between the rotor and motor.

Considering the elastic deformation of the traction shaft at the pinion position, the dynamic transmission error of the gear pair can be expressed as

$$\delta_{mi}=\begin{cases}\theta_{pi}R_p+\theta_{gi}R_g+(-1)^i\left(Z_{pi}+w_{pzi}-Z_{gi}\right)\cos\alpha_m\\ \quad -(-1)^i\left(X_{pi}+w_{pxi}-X_{gi}\right)\sin\alpha_m-b_0-e_i, & \text{for forward - side contact},\\ \theta_{pi}R_p+\theta_{gi}R_g+(-1)^i\left(Z_{pi}+w_{pzi}-Z_{gi}\right)\cos\alpha_m\\ \quad +(-1)^i\left(X_{pi}+w_{pxi}-X_{gi}\right)\sin\alpha_m-b_0-e_{ri}, & \text{for backward - side contact},\end{cases}\quad (i=1,2,3,4), \tag{21}$$

where θ_p/θ_g, R_p/R_g, X_p/X_g and Z_p/Z_g are the rotational speeds, base circle radii, longitudinal and vertical displacements of the pinion and gear, respectively; α_m, b_0, e_i and e_{ri} are the pressure angle, clearance, manufacture and assembly errors of the gear pair, respectively. The corresponding time-varying mesh stiffness can be calculated by an improved method proposed by Chen et al. in Refs. [39, 40].

A spatial dynamics model of the rolling bearing is established in Ref. [26], however, the elastic deformations of the components of the bearing are ignored. For overcoming this gap, an improved dynamics model of rolling bearing combining the rigid motions and elastic deformations of the roller and rings is developed. Besides, the contact stiffness K_{er} between the inner and outer races via the flexible roller considering the distortion of the roller and the effect of the lubricant oil is adopted to replace the corresponding equivalent contact stiffness K_e of an unlubricated bearing in this study. Considering the calculating efficiency of the simulation, the roll and yaw motions of the roller are not involved.

Consequently, the contact forces between the jth roller and inner/outer races can be expressed as

$$\begin{cases}N_{ij}=\chi_j K_{er}\delta_{ioj}^{10/9},\\ N_{oj}=N_{ij}+M_r\omega_{rj}^2R_m,\\ j=1,2,\cdots,n,\end{cases} \tag{22}$$

where M_r is the roller mass; ω_{rj} is the circumferential speed of jth roller; R_m is the pitch radius; n is the number of rollers; the calculating coefficient χ_j can be expressed as

$$\chi_j=\begin{cases}1 & \delta_{ioj}\geq 0,\\ 0 & \delta_{ioj}<0.\end{cases} \tag{23}$$

The relative radial displacement between the inner and outer rings at the angular position of jth roller can be expressed as

$$\begin{aligned}\delta_{ioj}=&X_{io}\cos\psi_{rj}+Z_{io}\sin\psi_{rj}+0.5\delta_{eij}+\delta_{di}\left(\psi_{rj}\right)\\ &+0.5\delta_{eij}+\delta_{do}\left(\psi_{rj}\right)+h_{cfij}+h_{cfoj}-\frac{e}{2},\end{aligned} \tag{24}$$

where ψ_{rj} is the angular position of jth roller; e is the radial clearance of bearing. It should be noted that the elastic deformation of jth roller has been considered in contact stiffness K_{er} according to Eq. (13), therefore, it is not involved in Eq. (24) for avoiding repetition.

The calculating equations for resultant forces of bearing and dynamic equations of the traction motor and rolling bearings can be referenced in Eqs. (34)–(41) in Ref. [26]. More detailed information about the locomotive-track coupled dynamics model and numerical integration method can be found in Refs. [26, 28–30].

3 Dynamic Simulation and Result Analysis

To analyze the elastic deformations of the rotor-bearing-pinion system and its effect on the dynamic responses of the traction motor and railway vehicle, the simulated results extracted from locomotive-track coupled dynamics models with rigid (RM) or flexible traction motor (FM) systems are compared in this study. The main dynamics and structure parameters of the HX locomotive, which is widely employed in Chinese railway, can be found in Ref. [26]. The operation speed of the locomotive is 80 km/h when the train is running along a straight line. The elastic deformations of the traction shaft at the rotor and pinion positions, the range of the rotor motion, and the dynamic eccentric distance are extracted. In addition, the dynamic forces acting on the traction motor, such as the centrifugal force of the rotor, UMP, mesh force, and roller-race contact forces of driving and non-driving end bearings, are displayed to reveal the effect of the elasticity of the rotor-bearing-pinion system on the dynamic characteristics of the traction motor. Besides, the vertical

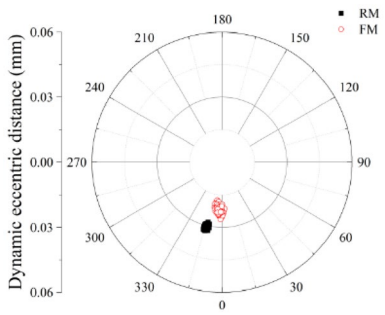

Figure 6 Range of rotor motion

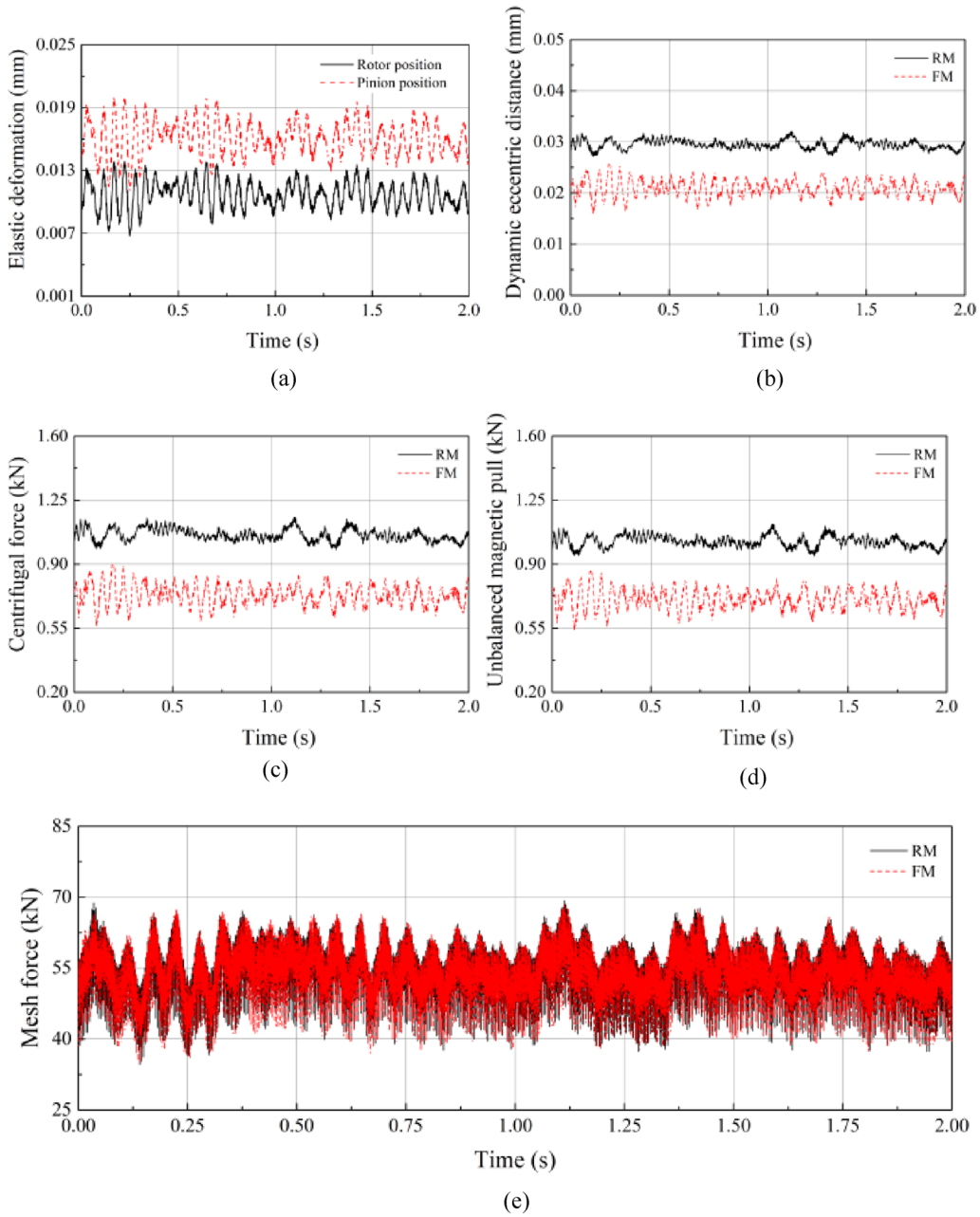

Figure 7 Effect of elasticity of shaft and support bearings on the internal dynamic forces of traction motor: **a** elastic deformations of the shaft, **b** dynamic eccentric distance of rotor, **c** centrifugal force of rotor, **d** UMP, and **e** mesh force

vibrations of the traction motor and connecting components, namely, the rotor, motor, wheelset and bogie frame, are extracted in this section.

3.1 Effect of Elasticity of Traction Shaft and Support Bearings

During the operation, the range of the rotor motion is obtained and illustrated in Figure 6. A measured track random irregularity [26] is used in this section. Under the effect of the wheel-rail impact induced by the track irregularity, the internal dynamic forces of traction motor, and time-varying mesh force, the longitudinal and vertical eccentric distances of rotor extracted from FM are shorter than that of RM. As illustrated in Figure 7, it can be seen that the elastic deformation of the shaft can not be ignored because of the comparable

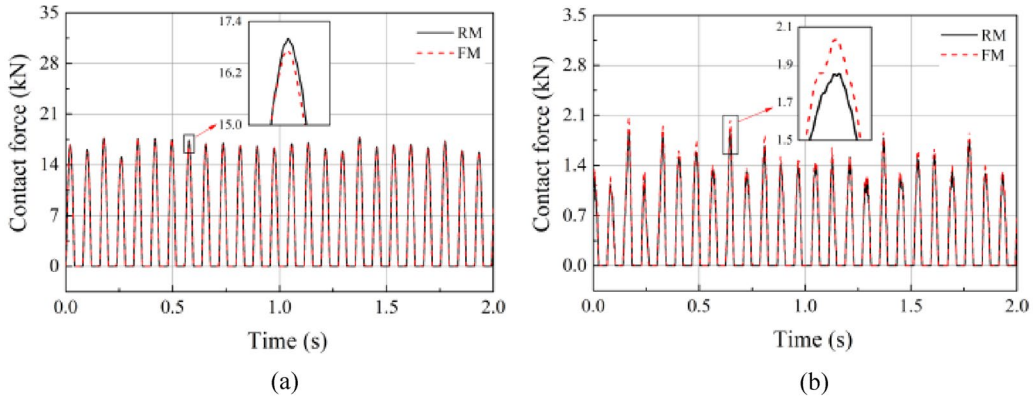

Figure 8 Contact forces between the roller and inner race of: **a** driving end baring, and **b** non-driving end bearing

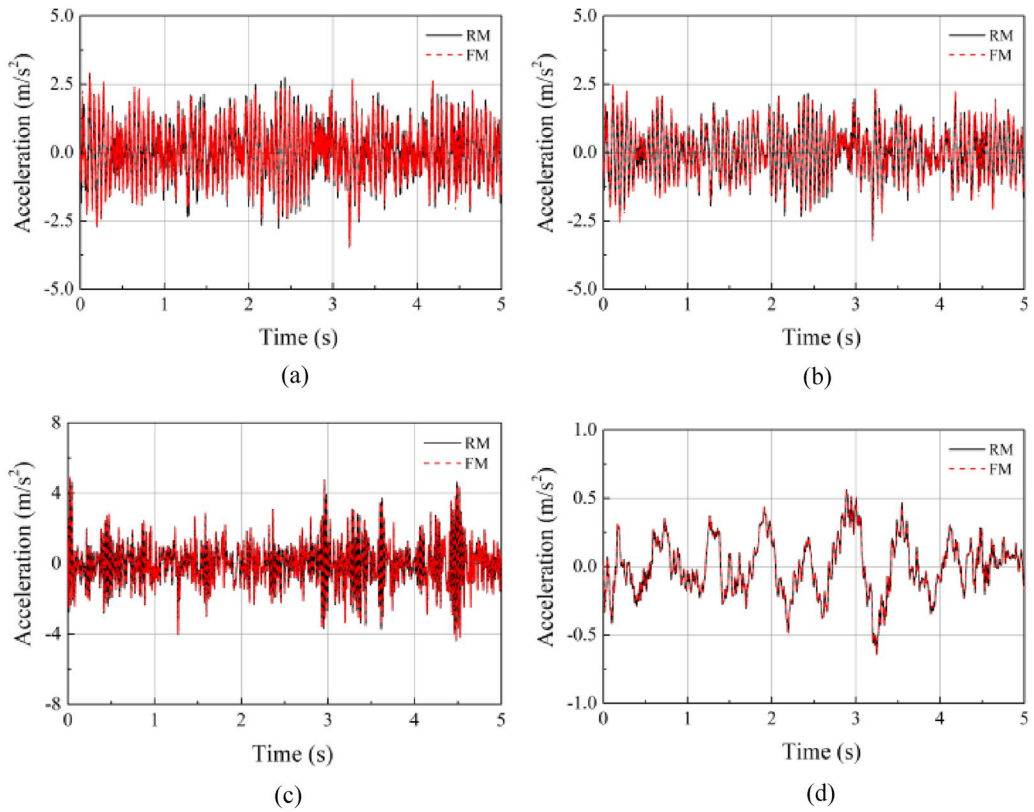

Figure 9 Vertical vibration responses of the vehicle system: **a** rotor, **b** motor, **c** wheelset, and **d** bogie

amplitudes compared with the relative displacement between the rotor and motor. The mean value of dynamic rotor eccentricity decreases about 1/3 with the elasticity of shaft and support bearings. Therefore, the mean value of the corresponding centrifugal force and UMP extracted from FM is about 2/3 of those from RM. Owing to the smaller dynamic loads of the rotor, the elastic deformations of components of bearing, and the change of the state of rotor motion, the roller-race contact force extracted from the driving end bearing is slightly smaller, while that from the non-driving end bearing is larger about 7.2%, which is illustrated in Figure 8. In addition, as illustrated in Figure 9, the elastic deformation of the shaft at the pinion position is larger

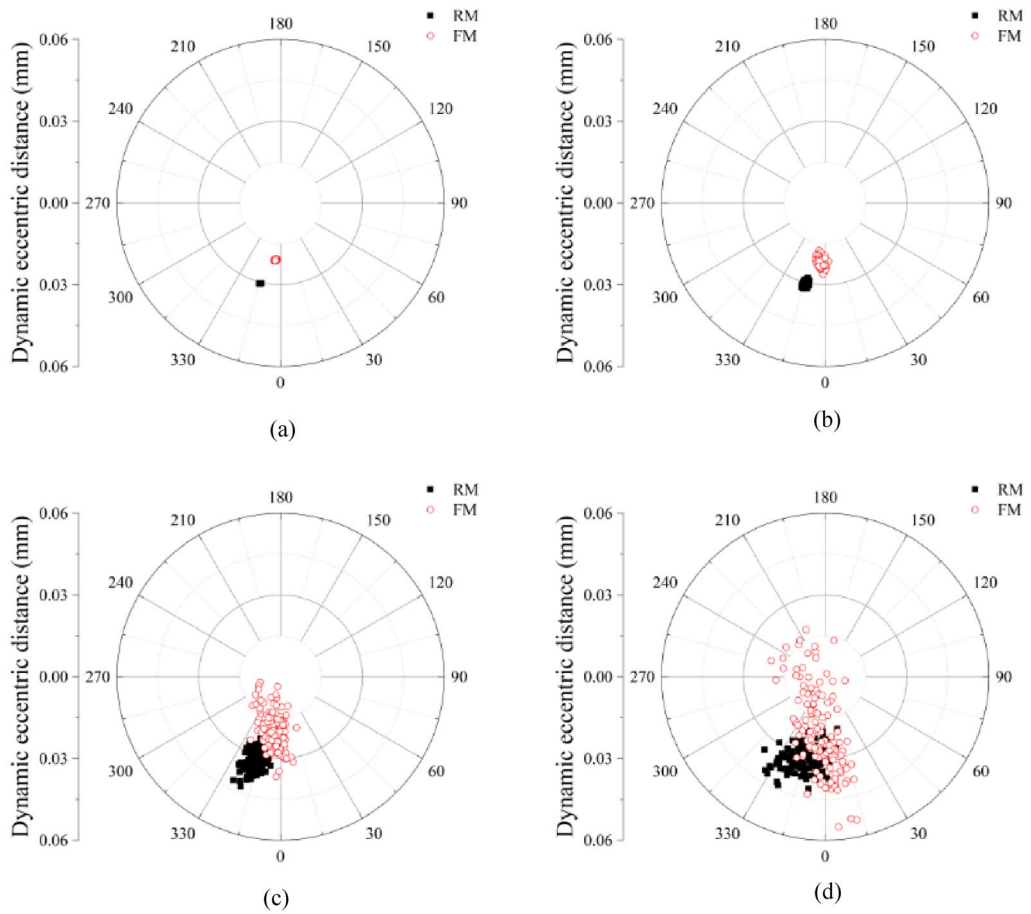

Figure 10 Effect of track irregularity on the range of rotor motion: **a** Case 1, **b** Case 2, **c** Case 3, and **d** Case 4

than that at the rotor position owing to the larger mesh force and gravity of the rotor. Moreover, it should be noted that the effect of the flexible traction motor system is weak for the dynamic characteristics of the locomotive with a healthy traction system. In conclusion, there is a certain difference between the dynamic characteristics of the traction motor described by RM and FM, which cannot affect the corresponding dynamic researches for the normal railway vehicle.

3.2 Effect of Track Irregularity

The track random irregularity is the major external excitation for the railway vehicle, which can significantly affect the service environment and working condition of the traction motor through the vibration transmission and gear engagement. According to the railway line status, four types of track irregularity (Case 1: no track irregularity, Case 2: measured track irregularity, Case 3: sixth-grade American track spectra, and Case 4: fifth-grade American track spectra) are used in this section, and they are successively worsening. The influences of wheel-rail impact induced by the track irregularity on dynamic characteristics of the traction motor are illustrated in Figures 10–12. As shown in Figure 11, the label DB is the driving end bearing, and NDB is the non-driving end bearing. It can be seen that with the deteriorating of line condition, the dynamic load and internal dynamic forces acting on the traction motor, namely, the mesh force, centrifugal force, and UMP, increase observably. The vibration of the rotor becomes more intense under the intensified wheel-rail interactions. This phenomenon will be more obvious considering the elastic structure deformation of the components of the traction motor, especially in the vertical direction. In addition, the vibrations of the traction motor and wheelset further intensify the interaction between the pinion and gear at the gear meshing interface. Therefore, the longitudinal vibration of the rotor is stronger with the deteriorating of the locomotive working condition. Meanwhile, the working conditions of motor bearings become unstable. As illustrated

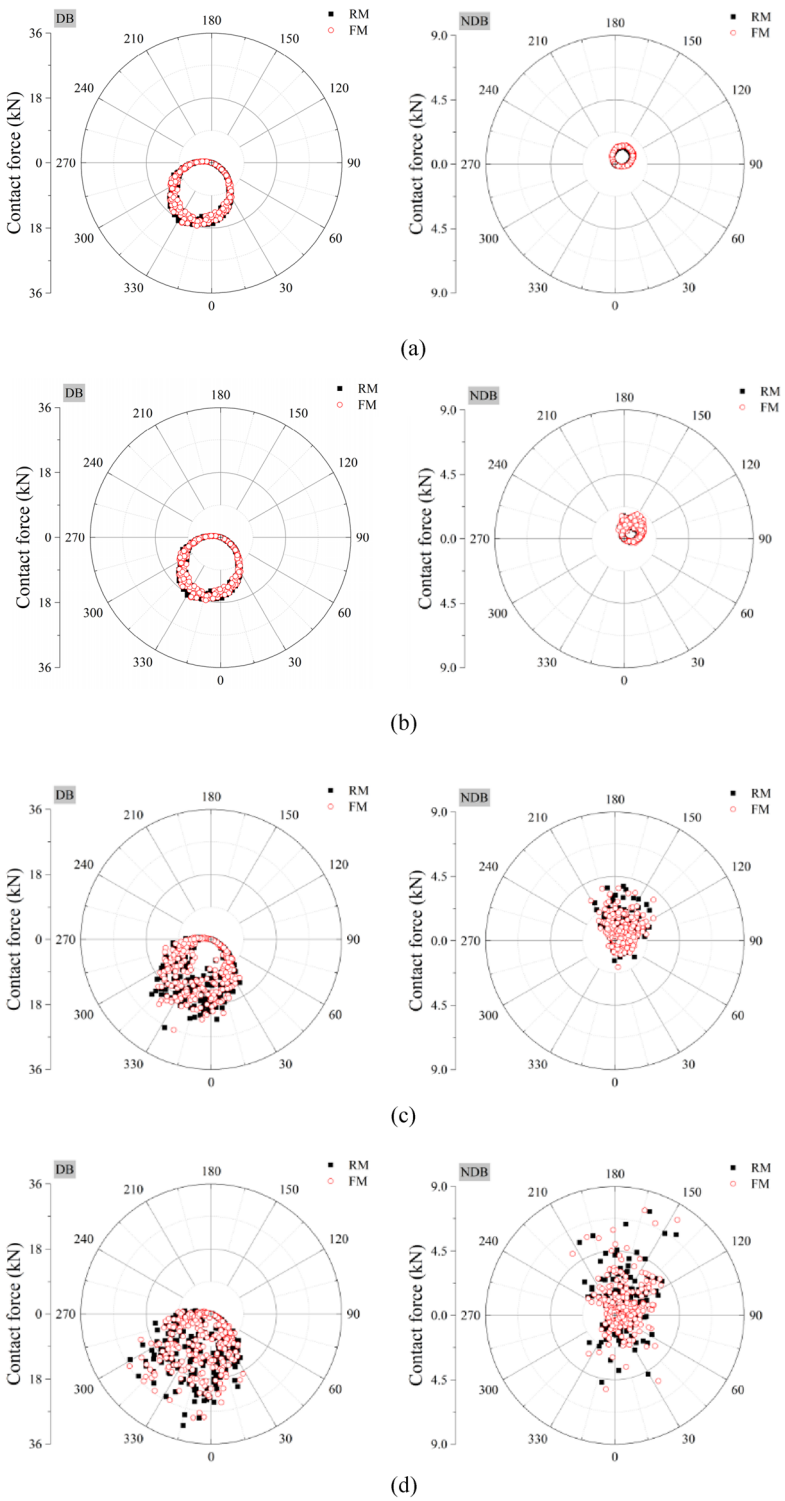

Figure 11 Effect of track irregularity on roller-race contact of driving and non-driving end bearings: **a** Case 1, **b** Case 2, **c** Case 3 and **d** Case 4

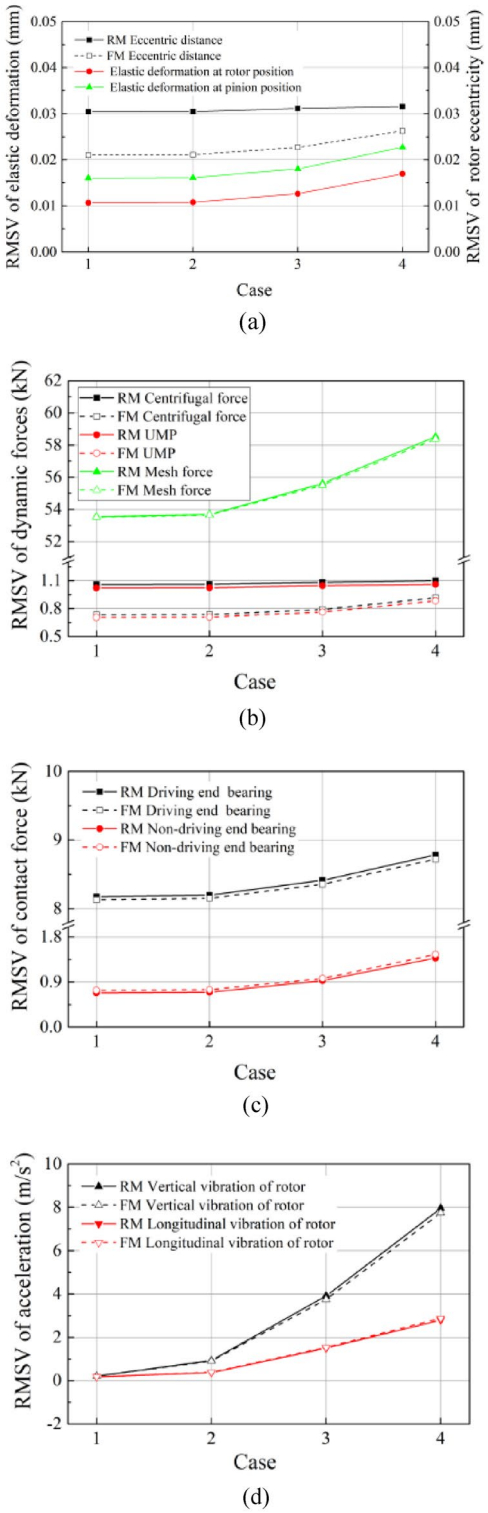

Figure 12 Effect of track irregularity on RMSV of: **a** dynamic rotor eccentricity and elastic deformation of the shaft, **b** dynamic forces of traction motor, **c** roller-race contact forces of motor bearings, and **d** vibration accelerations of the rotor

in Figure 11, under the violent impact generated from the wheel-rail interface, the frequent contact phenomenon occurs at the loaded region of driving end bearing, while the non-driving end bearing even cannot maintain a defined loaded region.

The corresponding statistical indicators of the dynamic forces, dynamic rotor eccentricity, and vibration are illustrated in Figure 12. As a joint result of the internal and external excitations, the root mean square values (RMSVs) of contact force between roller and race of motor bearings are gradually increasing. Moreover, the roller-race contact force of the driving end bearing extracted from the FM is slightly smaller than that of RM, while an opposite phenomenon occurs for the non-driving end bearing. According to Eq. (2), the elastic deformations of the traction shaft increase as the intensified wheel-rail interaction and gear meshing. The RMSVs of rotor eccentricity extracted from the FM are smaller than those of RM as the discussion in Section 2.1, while the difference value between them is decreased gradually, while the motion directions of rotors are markedly different. There is a significant difference between the RMSVs of elastic deformations of the shaft at rotor and pinion, whose reason is similar as mentioned earlier.

3.3 Effect of Rotor Eccentricity

The rotor eccentricity induced by the manufacturing and assembling errors, binding of the transmission shaft, radial clearance of support bearings and so on, can generate large centrifugal forces and UMP, and further influence the elastic deformation of the shaft, and deteriorate the working conditions of the traction motor. The initial eccentric distance of the rotor is given as 0 mm, 0.2 mm, 0.4 mm, 0.6 mm, 0.8 mm, and 1.0 mm, respectively. As illustrated in Figure 13, with the increase of the eccentric distance, the coincidence degree between the trajectories of the rotor extracted from RM and FM becomes worse owing to the bigger elastic structure deformations of the transmission shaft and support bearings under the larger radical forces. The effect of the rotor eccentricity on the motor bearings is significant. The roller-race contact forces and the corresponding contact angular position are illustrated in Figure 14. The loaded regions of the motor bearings expand with the increase of the rotor eccentricity, while the non-driving end bearing easily loses the defined loaded region. The effect of rotor eccentricity on the dynamic performances of motor bearings will be stronger considering the elastic deformations of the components of the traction motor.

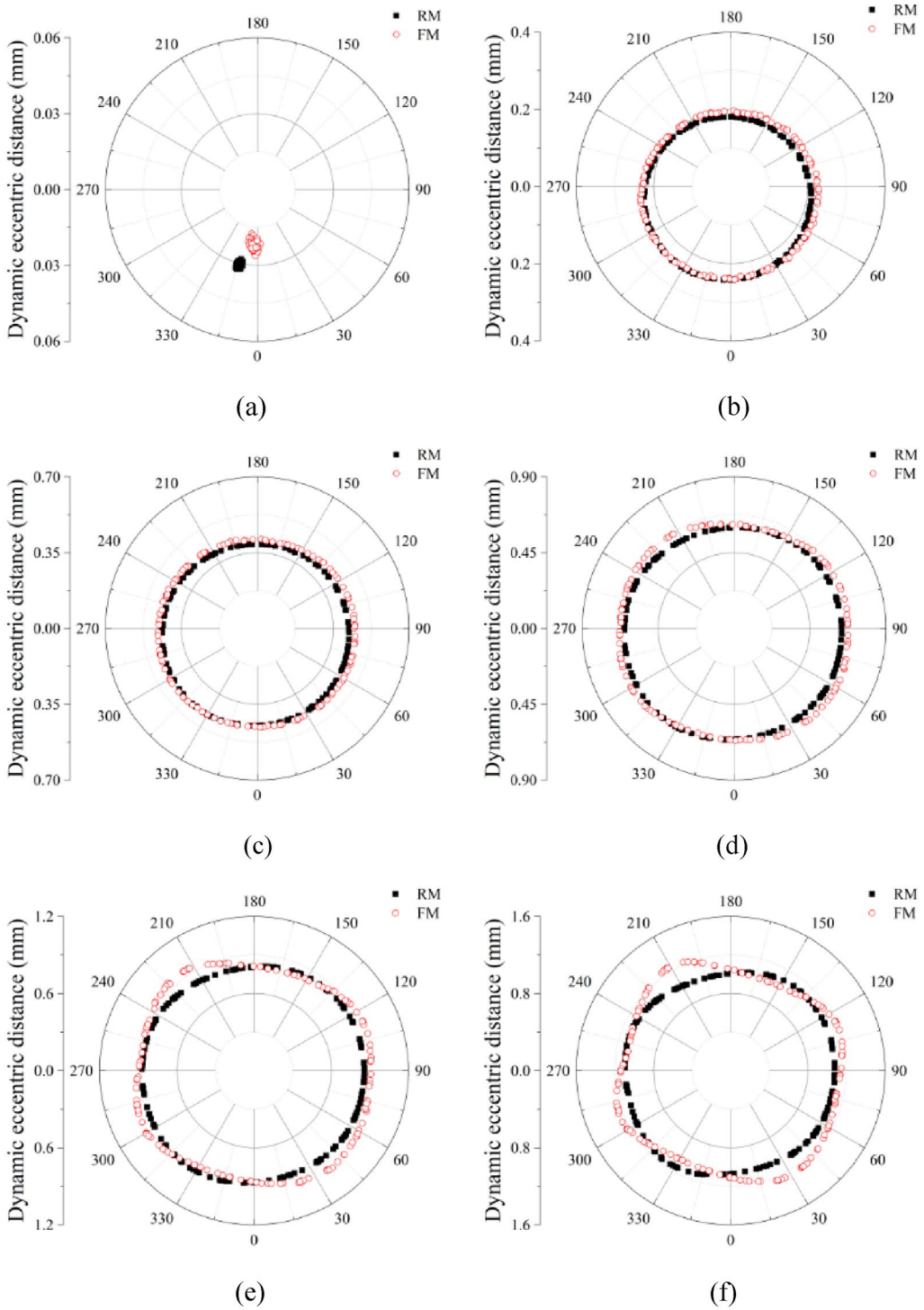

Figure 13 Effect of rotor eccentricity on range of rotor motion: **a** 0 mm, **b** 0.2 mm, **c** 0.4 mm, **d** 0.6 mm, **e** 0.8 mm, and **f** 1.0 mm

The effects of the rotor eccentricity on the RMSVs of the elastic deformation of the shaft, dynamic rotor eccentricity, dynamic forces of the traction motor, and vibration accelerations of the rotor are discussed in Figure 15. It can be seen that the RMSV of elastic deformation of the traction shaft at rotor position is smaller than that at pinion position with a shorter eccentric distance. When the initial eccentric distance

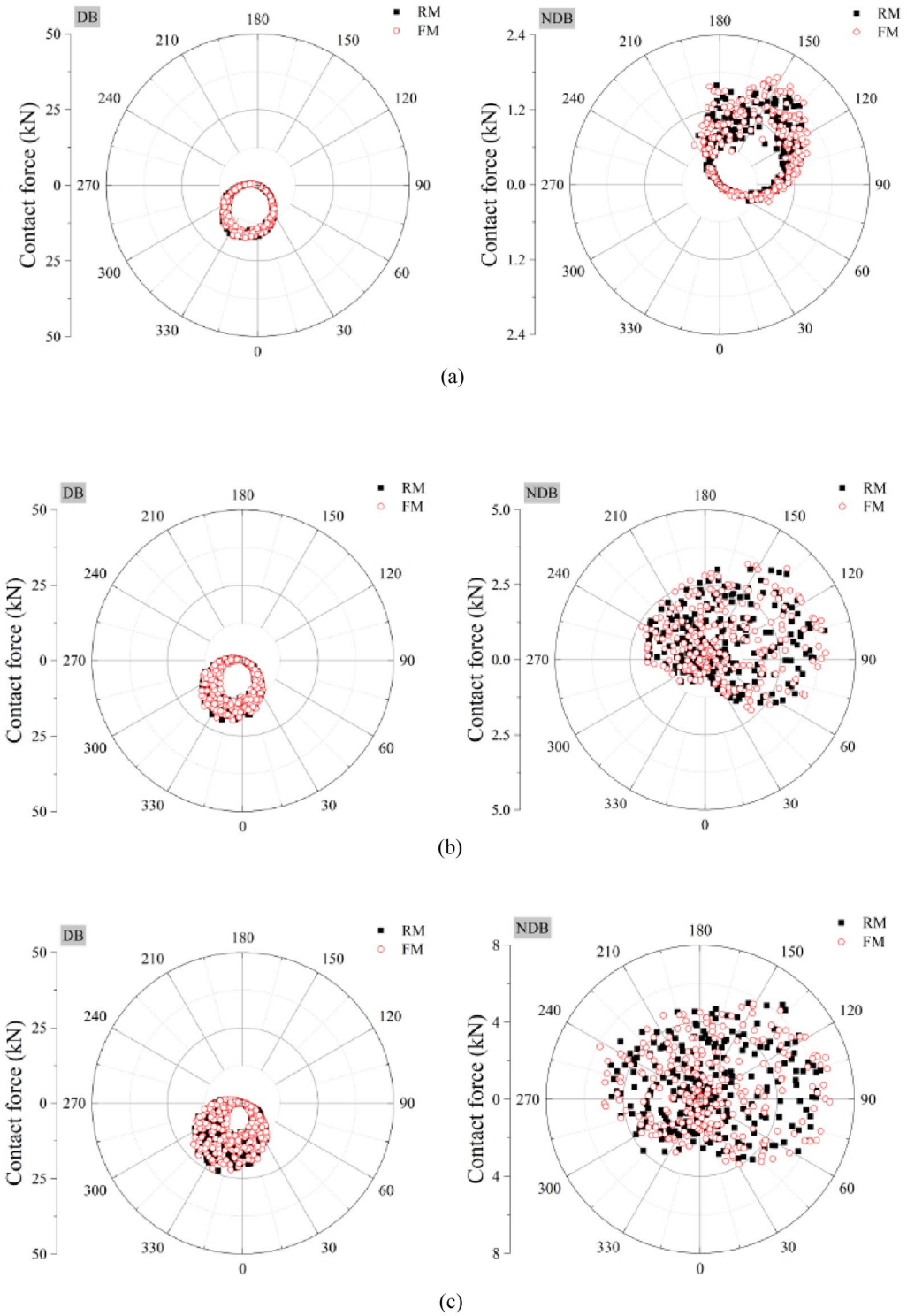

Figure 14 Effect of rotor eccentricity on roller-race contact forces of driving and non-driving end bearings: **a** 0 mm, **b** 0.2 mm, **c** 0.4 mm, **d** 0.6 mm, **e** 0.8 mm, and **f** 1.0 mm

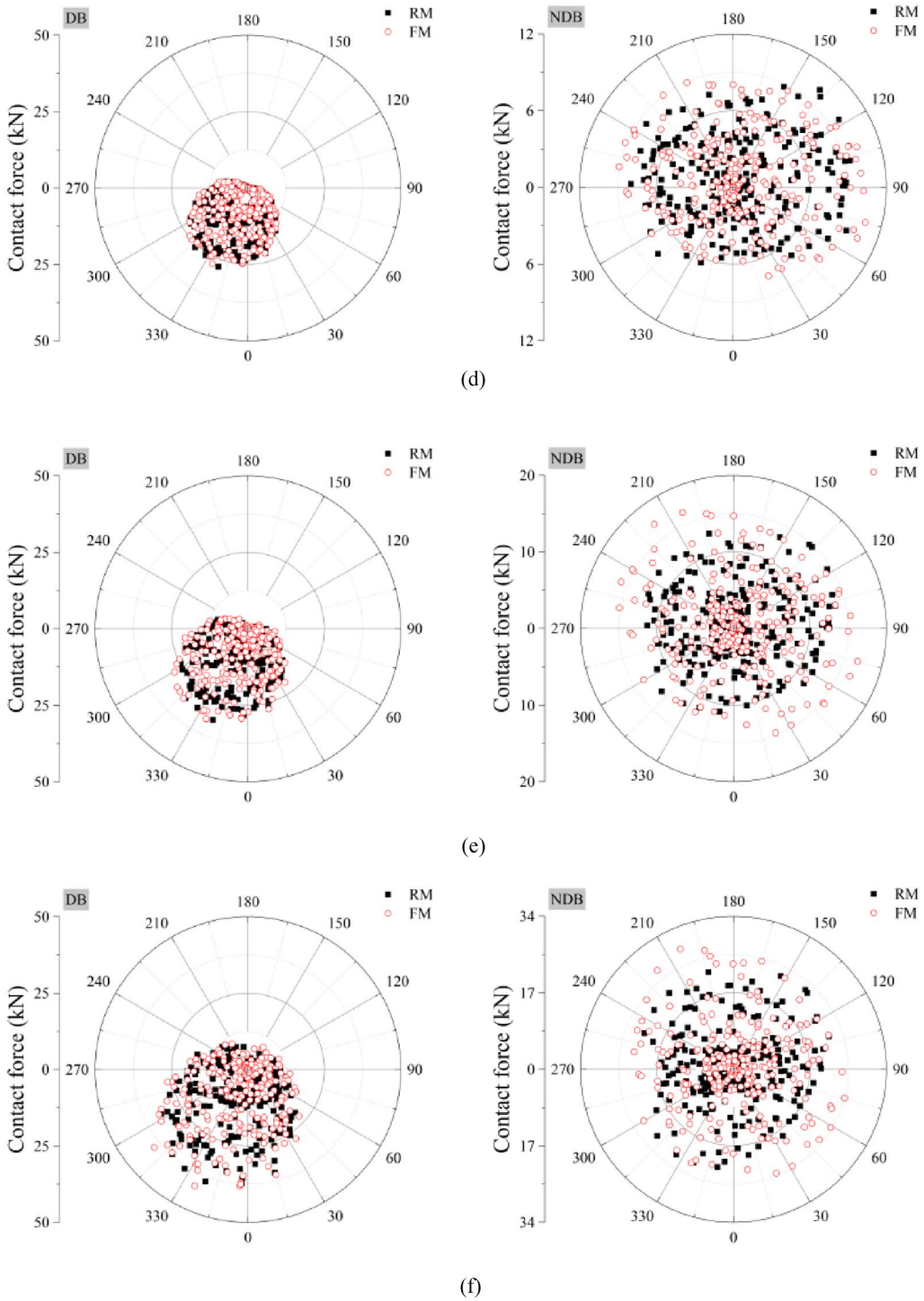

Figure 14 continued

is larger than 0.4 mm, an opposite phenomenon will happen. At the same time, there will be a big difference between the dynamic responses of the traction motor described as RM or FM models. Owing to the larger rotor eccentricity extracted from FM, the RMSVs of dynamic forces of the traction motor system, such as the centrifugal force, UMP, mesh force, and roller-race contact forces of driving and non-driving end bearings,

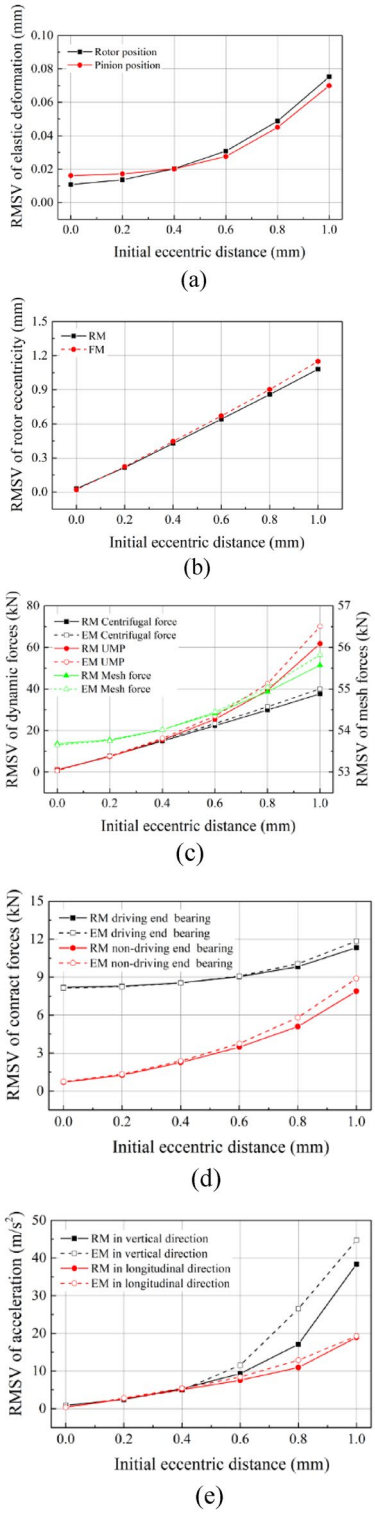

Figure 15 Effect of rotor eccentricity on the RMSVs of: **a** elastic deformation of the shaft, **b** dynamic eccentric distance of rotor, **c** internal dynamic forces of traction motor and mesh force, **d** roller-race contact forces of motor bearings, and **e** vibration accelerations of rotor

are larger than those of RM. A similar phenomenon generates at the vibration responses of the rotor and motor. In addition, if the initial eccentric distance is larger than the critical value (1.23 mm for RM and 1.15 mm for FM), the impact rub-impact phenomenon will deteriorate the working conditions of the traction motor and its neighboring components. Results underscore the role of the elasticity of traction shaft and support bearings in dynamic researches of the locomotive traction power transmission system with the growth of the eccentric distance.

4 Conclusions

An improved dynamics model of traction motor in a locomotive is established in this study by considering the elasticity of the rotor shaft and the support bearings. This model couples the kinetic equations of the rotor and its support bearings with the determination of elastic deformations. The effect of elastic deformations is considered in the rotor-motor interaction, roller-race connection, and gear engagement. In addition, the traction motor and the locomotive-track system are integrated via the hung rod, hugging bearings and gear transmission, and coupled through the vibration transmission and gear meshing. Results indicate that, for a locomotive with healthy traction motors, the elastic deformation of the shaft and the bearings could change the range of the rotor motion, and further reduce the dynamic rotor eccentricity, and further decrease the corresponding centrifugal force and UMP. Owing to the change of the motion state of the rotor, the roller-race contact force of the driving end bearing is slightly smaller compared with that extracted from RM, while an opposite phenomenon occurs for the non-driving end bearing. With the deterioration of the line condition, the wheel-rail interactions are intensified, and the vibration conditions of the rotor become more intense, especially in the vertical direction. Under the effect of the rotor eccentricity, it is essential to consider the elasticity of the traction shaft and support bearings because of the investigation of the dynamic characteristics of the faulted motor. Meanwhile, the critical value of the initial eccentric distance for the rub-impact phenomenon decreases from 1.23 mm to 1.15 mm. If the initial eccentric distance exceeds 0.4 mm, the elastic deformation of the shaft at the rotor position will be larger than that at the pinion position. Therefore, the results underscore the role of the elasticity of the traction shaft and support bearings in dynamic researches of the traction motor. Comparisons of the simulation results considering the effects of wheel-rail interaction and rotor eccentricity show that this improved flexible dynamics model is more accurate and rational than the rigid model in evaluating the dynamic characteristics of the traction motor.

Acknowledgements
Not applicable.

Author contributions
YL established the dynamic modelling, did simulation, and prepared the manuscript; ZC offered the project and assisted in analyses with JN; KW and WZ were in charge of the guidance and final check. All authors read and approved the final manuscript.

Authors' Information
Yuqing Liu, was born in Shanxi Province, China, in 1996. He is currently pursuing the Ph.D. degree with the *State Key Laboratory of Traction Power, Southwest Jiaotong University*. His research interests include bearing dynamics and vehicle-track coupled dynamics. E-mail: yuqing1012@my.swjtu.edu.cn
Zaigang Chen, was born in Sichuan Province, China, in 1984. He is a full professor and currently works at the *State Key Laboratory of Traction Power, Southwest Jiaotong University*. He does research in railway vehicle system dynamics and mechanical transmission dynamics and fault diagnosis. E-mail: zgchen@home.swjtu.edu.cn
Jieyu Ning, was born in Anhui Province, China, in 1996. She is currently pursuing the Ph.D. degree with the *State Key Laboratory of Traction Power, Southwest Jiaotong University*. Her research interests include gear dynamics and fault diagnosis. E-mail: jyning@my.swjtu.edu.cn
Kaiyun Wang, was born in Jiangxi Province, China, in 1974. He is the Director of *State Key Laboratory of Traction Power, Southwest Jiaotong University at Chengdu, China*. His research interest is on railway system dynamics, focusing on vehicle-track coupled dynamics, train longitudinal dynamics. E-mail: kywang@swjtu.edu.com.
Wanming Zhai, was born in Jiangsu Province, China, in 1963. He is the Director of *Train and Track Research Institute, State Key Laboratory of Traction Power, Southwest Jiaotong University at Chengdu, China*. His research interest is on railway system dynamics, focusing on vehicle-track coupled dynamics, train-track-bridge interaction. He is a Member of Chinese Academy of Science and International Member of US National Academy of Engineering (NAE). He is the Editor-in-Chief of Railway Engineering Science and International Journal of Rail Transportation. E-mail: wmzhai@swjtu.edu.cn

Funding
Supported by National Natural Science Foundation of China (Grant Nos. 52022083, 51775453, and 51735012).

Competing Interests
The authors declare no competing financial interests.

Received: 20 October 2021 Revised: 25 April 2022 Accepted: 10 June 2022
Published online: 14 July 2022

References
[1] W M Zhang, G Meng, D Chen, et al. Nonlinear dynamics of a rub-impact micro-rotor system with scale-dependent friction model. *Journal of Sound and Vibration*, 2008, 309(3-5): 756-777.
[2] J G Wang, R Sun, M Q Ren, et al. Nonlinear characteristics of rubbing rotor–bearing system of locomotive excited by rotating speed of the traction motor. *IOP Conference Series: Earth and Environmental Science*. IOP Publishing, 2019, 242(3): 032054.
[3] P K Gupta. Transient ball motion and skid in ball bearings. *Journal of Lubrication Technology*. 1971, 97(2): 261-269.
[4] H S Yang, G D Chen, S Deng, et al. Rigid-flexible coupled dynamic simulation of aeroengine main-shaft high speed cylindrical roller bearing. *2010 3rd International Conference on Advanced Computer Theory and Engineering (ICACTE)*, Chengdu, August 2010, 4: 31-35.
[5] Y Q Liu, Z G Chen, L Tang, et al. Skidding dynamic performance of rolling bearing with cage flexibility under accelerating conditions. *Mechanical Systems and Signal Processing*, 2021, 150: 107257.
[6] J Liu, Y J Xu, G Pan. A combined acoustic and dynamic model of a defective ball bearing. *Journal of Sound and Vibration*, 2021, 501: 116029.
[7] A B Jones. A general theory for elastically constrained ball and radial roller bearings under arbitrary load and speed conditions. *Journal of Basic Engineering*, 1960, 82(2): 309-320.
[8] C Machado, M Guessasma, E Bellenger. An improved 2D modeling of bearing based on DEM for predicting mechanical stresses in dynamic. *Mechanism and Machine Theory*, 2017, 113: 53-66.
[9] J Liu, H Wu, Y M Shao. The influence of the raceway thickness on the dynamic performances of a roller bearing. *The Journal of Strain Analysis for Engineering Design*, 2017, 52(8): 528-536.
[10] J Liu, C K Tang, Y M Shao. An innovative dynamic model for vibration analysis of a flexible roller bearing. *Mechanism and Machine Theory*, 2019, 135: 27-39.
[11] A Leblanc, D Nelias, C Defaye. Nonlinear dynamic analysis of cylindrical roller bearing with flexible rings. *Journal of Sound and Vibration*, 2009, 325(1-2): 145-160.
[12] F F Ehrich, J J O'Connor. Stator whirl with rotors in bearing clearance. *Journal of Manufacturing Science and Engineering*, 1967, 89(3):381-389.
[13] F F Ehrich. Observations of nonlinear phenomena in rotordynamics. *Journal of System Design and Dynamics*, 2008, 2(3): 641-651.
[14] C Villa, J J Sinou, F Thouverez. Stability and vibration analysis of a complex flexible rotor bearing system. *Communications in Nonlinear Science and Numerical Simulation*, 2008, 13(4): 804-821.
[15] M L Shi, D Z Wang, J G Zhang. Nonlinear dynamic analysis of a vertical rotor-bearing system. *Journal of Mechanical Science and Technology*, 2013, 27(1): 9-19.
[16] P K Gupta. *Advanced dynamics of rolling elements*. New York: Springer, 2012.
[17] Y M Li, H R Cao, L K Niu, et al. A general method for the dynamic modeling of ball bearing–rotor systems. *Journal of Manufacturing Science and Engineering*, 2015, 137: 021016.
[18] X Tan, J C He, X Chen, et al. Dynamic modeling for rotor-bearing system with electromechanically coupled boundary conditions. *Applied Mathematical Modelling*, 2021, 91: 280-296.
[19] J J Zhang, L K Zhang, Z Y Ma, et al. Coupled bending-torsional vibration analysis for rotor-bearing system with rub-impact of hydraulic generating set under both dynamic and static eccentric electromagnetic excitation. *Chaos, Solitons & Fractals*, 2021, 147: 110960.
[20] G H Huang, N Zhou, W Zhang. Effect of internal dynamic excitation of the traction system on the dynamic behavior of a high-speed train. *Proceedings of the Institution of Mechanical Engineers, Part F: Journal of Rail and Rapid Transit*, 2016, 230(8): 1899-1907.
[21] W M Zhai, K Y Wang, C B Cai. Fundamentals of vehicle–track coupled dynamics. *Vehicle System Dynamics*, 2009, 47(11): 1349-1376.
[22] Z G Chen, W M Zhai, K Y Wang. Vibration feature evolution of locomotive with tooth root crack propagation of gear transmission system. *Mechanical Systems and Signal Processing*, 2019, 115: 29-44.
[23] Y W Yu, L L Zhao, C C Zhou. Effect of vehicle-track vertical coupling vibrations on frame-mounted traction motor dynamics. *Journal of Vibroengineering*, 2020, 22(1): 184-196.
[24] [Z W Zhou, Z G Chen, M Spiryagin, et al. Dynamic response feature of electromechanical coupled drive subsystem in a locomotive excited by wheel flat. *Engineering Failure Analysis*, 2021, 122: 105248.
[25] T T Wang, Z W Wang, D L Song, et al. Effect of track irregularities of high-speed railways on the thermal characteristics of the traction motor bearing. *Proceedings of the Institution of Mechanical Engineers, Part F: Journal of Rail and Rapid Transit*, 2021, 235(1): 22-34.
[26] Y Q Liu, Z G Chen, K Y Wang, et al. Dynamic modelling of traction motor bearings in locomotive-track spatially coupled dynamics system. *Vehicle System Dynamics*, 2021. https://doi.org/10.1080/00423114.2021.1918728.
[27] Y Q Liu, Z G Chen, W Li, et al. Dynamic analysis of traction motor in a locomotive considering surface waviness on races of a motor bearing. *Railway Engineering Science*, 2021, 29(4): 379-393.
[28] T Zhang, Z G Chen, W M Zhai, et al. Establishment and validation of a locomotive–track coupled spatial dynamics model considering dynamic effect of gear transmissions. *Mechanical Systems and Signal Processing*, 2019, 119: 328-345.
[29] Y Q Liu, Z G Chen, W M Zhai, et al. Dynamic investigation of traction motor bearing in a locomotive under excitation from track random geometry irregularity. *International Journal of Rail Transportation*, 2022, 10(1): 72-94.

[30] Y Q Liu, Z G Chen, K Y Wang, et al. Surface wear evolution of traction motor bearings in vibration environment of a locomotive during operation. *SCIENCE CHINA Technological Sciences*, 2022. https://doi.org/10.1007/s11431-021-1939-3.
[31] D X Chen. *Mechanical design hand book, Part 1*. Beijing: China Machine Press, 2007.
[32] H Cao. Research on digital modeling theory of high-speed machine tool spindles and its application. Xi'an: Xi'an Jiaotong University, 2010. (in Chinese)
[33] J Q Chen, H B Mao, B S Zhang. Theory study on hollow cylindrical roller bearing without preload. *Bearing*, 2002, 6: 1–5, 46. (in Chinese)
[34] H Aramaki, Y Shoda, Y Morishita, et al. The performance of ball bearings with silicon nitride ceramic balls in high speed spindles for machine tools. *ASME J. Tribol*, 1988, 110(4): 693-698.
[35] G Cavallaro, D Nelias, F Bon. Analysis of high-speed intershaft cylindrical roller bearing with flexible rings. *Tribology Transactions*, 2005, 48(2): 154-164.
[36] D Dowson, G Higginson. Elastohydrodynamic lubrication (SI Edition). Britain, Pergamon Press Ltd., 1977.
[37] S T Zhou, J W Zhu, Q Xiao, et al. Initial static eccentricity and gravity load on rotor orbit of EMU traction motor. *Journal of Mechanical Engineering*, 2020, 56(17): 145-154. (in Chinese)
[38] Y Q Liu, Z G Chen, X Hua, et al. Effect of rotor eccentricity on the dynamic performance of a traction motor and its support bearings in a locomotive. *Proceedings of the Institution of Mechanical Engineers, Part F: Journal of Rail and Rapid Transit*, 2022. https://doi.org/10.1177/09544097211072335.
[39] Z G Chen, Z W Zhou, W M Zhai, et al. Improved analytical calculation model of spur gear mesh excitations with tooth profile deviations. *Mechanism and Machine Theory*, 2020, 149: 103838.
[40] Z G Chen, J Y Ning J, K Y Wang, et al. An improved dynamic model of spur gear transmission considering coupling effect between gear neighboring teeth. *Nonlinear Dynamics*, 2021, 106(1): 339-357.